Fuel 419 (2026) 138901

Contents lists available at ScienceDirect

Fuel

journal homepage: www.elsevier.com/locate/fuel

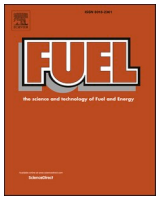

Full Length Article

Methane enrichment from $CH_4 + CO_2$ gas mixture via structure II clathrate hydrate: A continuous separation experiment for biogas upgrading

Meku Maruyama [a,*], Satoshi Takeya [b], Judith M. Schicks [c], Ryo Ohmura [a]

[a] Department of Mechanical Engineering, Keio University, 3-14-1 Hiyoshi, Kohoku-ku, 223-8522 Yokohama, Kanagawa, Japan
[b] National Institute of Advanced Industrial Science and Technology (AIST), Tsukuba West, 16-1, Onogawa, Tsukuba 305-8569, Japan
[c] GFZ Helmholtz Centre for Geosciences, Telegrafenberg, 14473 Potsdam, Germany

ARTICLE INFO

Keywords:
Clathrate hydrate
Biogas upgrading
Biomethane
Gas separation
Gas chromatography
Powder X-ray diffraction

ABSTRACT

Toward the widespread adoption of biomass energy for carbon neutral age, demand for biogas separation technologies that enables easier operation and maintenance is increasing. CH_4 enrichment in biogas in solid structure II clathrate hydrate has recently attracted attention, yet the knowledge is limited to the batch-type operation, which is far from engineering practice. In the present study, we have conducted hydrate-based CH_4 enrichment experiments with semi-batch and continuous separation methods in $CH_4 + CO_2$ + tetrahydropyran (THP) + water system, which are closer to applied-side operations. Semi-batch CH_4/CO_2 separation experiment with powder X-ray diffraction (PXRD) measurement revealed that CH_4 is enriched in the hydrate phase with its mole fraction from 0.60 to 0.81 via the formation of structure II hydrate with THP. The continuous CH_4/CO_2 separation experiment showed that CH_4 is concentrated in the hydrate slurry during the continuous formation process. The concentration of CH_4 in the hydrate slurry reached 0.65 in mole fraction at the steady state at $t = 24$ h from 0.45 at $t = 1$h. The experimental results of time-dependent changes in the compositions in the gas phase as well as in the hydrate slurry exhibited that the long-term operation of hydrate-based CH_4 enrichment was achieved and therefore could be implemented on a continuous industrial scale. The overall results demonstrated that the continuous CH_4 enrichment in biogas is an applicable scheme utilizing structure II hydrate.

1. Introduction

The transition to a carbon neutral society is being actively promoted in every field of industry. In 2016, the Paris Agreement was negotiated worldwide for mitigating climate change [1]. In 2018, a strategic vision called “A Clean Planet for all” was proclaimed by the EU commission, targeting an achievement of carbon neutral economy by 2050 [2]. In terms of fuel policy, the demand for sustainable fuels which do not increase CO_2 in the atmosphere during combustion is increasing. One approach to substituting fossil fuels is the biomass resources, which are biological materials involving sewage sludge, livestock manure, and municipal waste [3–5]. Biomass is utilized in the form of biogas obtained through methane fermentation process with its main components being around 60 % of methane (CH_4) and 40 % of carbon dioxide (CO_2) [6–9]. To adjust the calorific value according to the end-use of the biogas, the enrichment of CH_4 in biogas should be applied, a process called biogas upgrading [3]. Currently, pressure swing adsorption (PSA) technology is mainly applied to biogas upgrading [10–12]. However, PSA necessitates several columns for biogas compression and depressurization [13] as well as an independent procedure for H_2S removal [14], accordingly complex process and frequent maintenance. An alternative separation technique using clathrate hydrate provides a solution to the above existing problems. Furthermore, the energy consumption for hydrate-based CO_2 gas separation is estimated to be between 0.66 and 1.75 GJ/ton CO_2. This is known to be comparable to or even lower than that of other existing technologies, such as chemical absorption and membrane separation (over 2.0 GJ/ton CO_2) [15].

Clathrate hydrates (also known as gas hydrates, hereafter abbreviated as hydrates) are crystalline compounds with ice-like appearances having a large capacity of gas storage composed of a lattice of host water molecules encaging gaseous or organic guest molecules within its cavities. The host water molecules assemble the diverse crystallographic hydrate structures which depend on the geometry of the guest molecules. Hydrates with structures I, II, and H have widely been known as canonical structures, with each structure having its own geometry of cavities in the unit cell. The basic principle for hydrate-based mixed gas

* Corresponding author.
E-mail address: meku_selanjulio@keio.jp (M. Maruyama).

https://doi.org/10.1016/j.fuel.2026.138901
Received 12 October 2025; Received in revised form 28 January 2026; Accepted 22 February 2026
Available online 25 February 2026

separation is the guest selectivity of hydrate. The guest selectivity can be estimated from the difference in thermodynamic stability of hydrates. For example, structure I CO_2 hydrate forms at 277 K at 2 MPa [16], whereas the formation of structure I CH_4 hydrate requires a lower temperature below 265 K at the same pressure [17]. Considering CH_4 + CO_2 mixed gas separation, previous experimental studies have demonstrated that CO_2 is preferentially incorporated in the structure I hydrate phase, while CH_4 is enriched in the gas phase [18–22]. In the formation of hydrates of structure II with a large molecular guest compound, however, structure II hydrates that contain CH_4 are thermodynamically more stable than structure II hydrates that contain CO_2. For instance, equilibrium conditions for the formation of CH_4 + tetrahydropyran (THP) hydrate and CO_2 + THP hydrate are 290 K and 286 K, respectively, at 2 MPa [23]. The inversion in the phase equilibrium conditions for CH_4-containing and CO_2-containing structure II-hydrate-forming systems may be used for selective CH_4 separation. Lee et al. [24] investigated the phase equilibria of CH_4 + tetrahydrofuran (THF) + water, CO_2 + THF + water and CH_4 + CO_2 + THF + water systems. They were the first to imply the concentration of CH_4 in structure II hydrate phase in CH_4 + CO_2 + THF + water system. Seo et al. [25] achieved separation experiments using multi-stage batch reactors in two structure II-hydrate-forming systems of CH_4 + CO_2 + *tert*-butyl alcohol + water and CH_4 + CO_2 + trimethylene oxide + water. Their investigation showed that CH_4 enrichment from CH_4 + CO_2 gas mixture in the hydrate phase from 50 mol% to 85 mol% can be achieved through four- or five-stage batch operation utilizing structure II hydrate.

From the applied-side perspective, batch tests are insufficient to conclude that structure II-hydrate-forming system can be used for practical CH_4 enrichment in biogas. As mentioned above, structure II hydrates have potential as biogas upgrading material, but there is still no direct evidence showing the practicability of gas separation. Continuous separation experiments need to be conducted to demonstrate that the hydrate-based system works; while batch operation involves several series of reactors to obtain purified gas, in the continuous operation, a set of procedures starting from the formation of hydrate, via the discharge and transportation of the hydrate slurry to the hydrate decomposition can be achieved only within a series of reactors. Consequently, all of the above procedures can be concurrently performed. The capital investments for plant construction and the operation can therefore be reduced by launching the continuous separation process. To demonstrate that hydrate-based separation technology is applicable to an industrial-scale equipment, continuous separation experiments are essential. This is because only through the experiments can it be clarified whether the target hydrate-forming system can experimentally reach a steady state in a continuous process, and what values the compositions of the gas phase and the hydrate slurry will reach at the steady state. Until now, hydrate-based continuous separation experiments of CO_2 have been tested from CH_4 + CO_2 gas mixture [19], H_2 + CO_2 gas mixture [15,26,27], and N_2 + CO_2 gas mixture [28]. However, there is currently no report of continuous enrichment of CH_4 from CH_4-containing gas mixture. The achievement of continuous CH_4/CO_2 separation will take advantage over the PSA technology by reducing the number of reactors for biogas compression and depressurization. In addition, it has been revealed in simulation by Akatsu et al. [29] that H_2S removal from gas mixtures can be achieved at an early stage of continuous hydrate formation, indicating non-necessity of independent H_2S removal procedure unlike PSA.

In this study, hydrate-based continuous CH_4 separation experiment from CH_4 + CO_2 gas mixture was carried out with a goal of biogas upgrading. THP was used for structure II hydrate formation as a thermodynamic promoter. Among diverse guest compounds forming structure II hydrates, THP has been proposed as a practicable guest for industrial use for its partial solubility in water [15,23]. While guest compounds such as cyclopentane and tetrahydrofuran (THF) are known to significantly stabilize structure II hydrates, their industrial application is hampered by practical drawbacks. The low solubility of cyclopentane to water could result in the slow formation kinetics [30]. THF is known as one of the critical air pollutants that poses severe environmental and health risks [31]. In particular, THF is classified by the International Agency for Research on Cancer (IARC) as a Group 2B carcinogen, in other words, cancer-causing agent to humans [32]. In view of these issues, THP emerges as a safer alternative guest compound, as it is not identified as a hazardous air pollutant. In the experiments, the time evolutions of gas composition in the gas phase and in the hydrate slurry were continuously measured. Semi-batch experiment for CH_4/CO_2 separation was separately performed to investigate the composition in the hydrate phase. To determine the crystalline structure of hydrate obtained in the semi-batch experiment, powder X-ray diffraction (PXRD) was performed. Based on the above experimental attempts, the practicability of hydrate-based continuous CH_4 enrichment in biogas was evaluated.

2. Experimental section

2.1. Materials

The feed gas utilized in the experiment was CH_4 + CO_2 mixed gas with its certified molar ratio of CH_4: CO_2 = 0.600: 0.400 (synthesized by Taiyo Nippon Sanso JFP Co.). Liquid samples were THP (98.0 mass%, Tokyo Chemical Industry Co., Ltd.) and the laboratory-made distilled water. The same samples were used for both semi-batch as well as the continuous separation experiments.

2.2. Semi-batch CH_4/CO_2 separation with PXRD analysis

The semi-batch method is a method of producing a product by setting some species of the necessary materials in a mixing tank and then continuously supplying the remaining materials. The semi-batch apparatus used in this study is described in Fig. 1. The hydrate-forming reactor with an inner volume of 200 cm^3 was charged with 30.2 g of liquid water and 8.5 g of liquid THP with prescribed stoichiometric ratio of structure II hydrate (the mass fraction of THP, w_{THP} = 0.22). Since THP is partially soluble in water, the phase separation occurs in the aqueous phase into (i) liquid water saturated with THP and (ii) liquid THP saturated with water. The reactor was evacuated by using a vacuum pump and then pressurized with the CH_4 + CO_2 gas mixture up to 3.0 MPa at 285.1 K. Fig. 2 shows phase equilibrium points of CH_4 + THP hydrate [23], CO_2 + THP hydrate [23], CH_4 simple hydrate [17], CO_2 simple hydrate [16,17] and the experimental conditions in this study. The experimental condition of this study, p = 3.0 MPa and T = 285.1 K (half rhombus in Fig. 2), was chosen such that the CO_2 partial pressure (empty rhombus in Fig. 2) falls outside of the CO_2 + THP hydrate stability region (the higher-pressure and/or lower-temperature region than the empty circles in Fig. 2), while the CH_4 partial pressure (filled rhombus in Fig. 2) lies within the CH_4 + THP hydrate stability region (the higher-pressure and/or lower-temperature region than the filled circles in Fig. 2). The experimental condition also lies outside of the stability region of CO_2 simple hydrate.

After the agitation inside the reactor started with a magnetic stirrer at 100 rpm, the formation of hydrate was detected by a pressure decrease. The decrease in pressure denoted that the gas was encased into the hydrate structure. The reactor was repeatedly recharged with CH_4 + CO_2 gas mixture to 3.0 MPa until no further pressure decrease was observed. The total volume of gas consumption during the entire semi-batch hydrate formation was measured by collecting records of the decrease in system pressure. After the pressure reached a steady state, indicating that the maximal amount of water and THP in the reactor were converted into hydrate, the reactor was cooled below 253 K. The crystal sample was collected from the reactor. The sample of hydrate crystals was finely powdered below 100 K immediately after the cooling of the reactor. To measure the CH_4: CO_2 composition of hydrate and identify the crystalline hydrate structure, experiments with the obtained

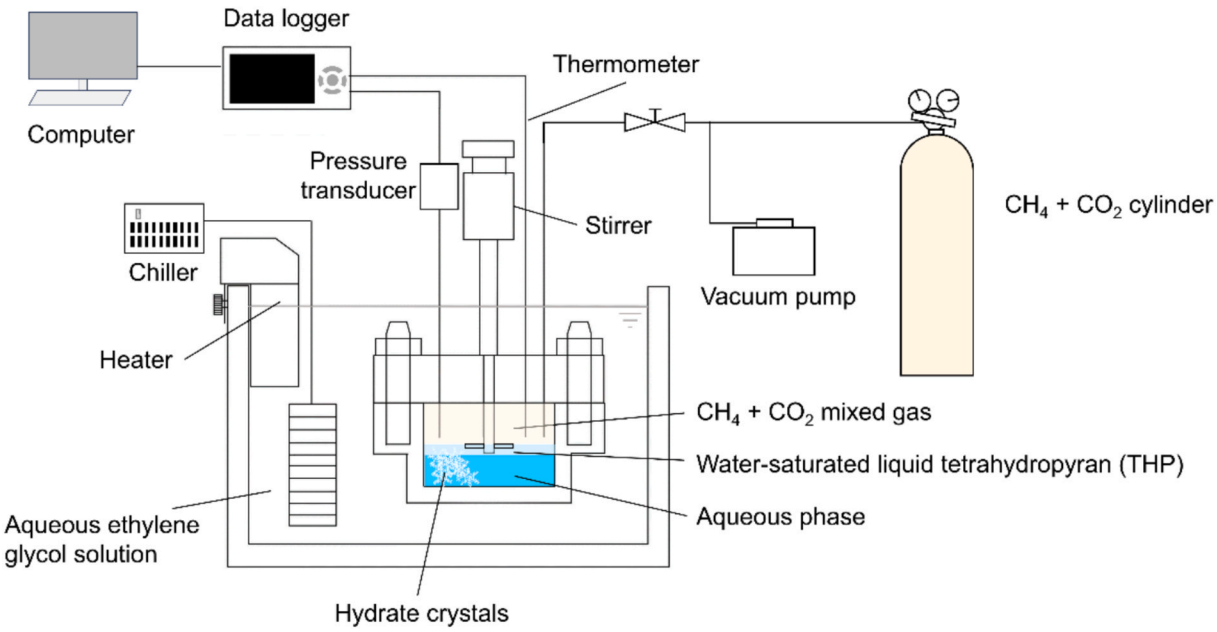

Fig. 1. Layout of the apparatus for hydrate-based semi-batch CH_4/CO_2 separation experiment.

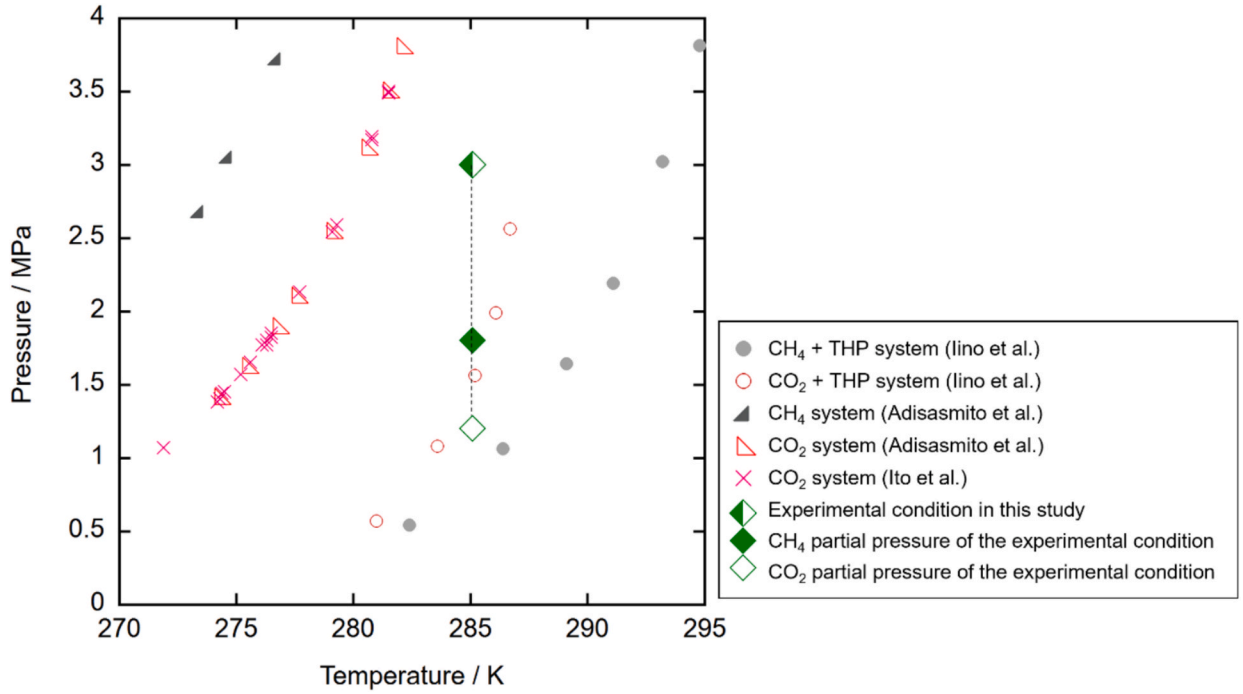

Fig. 2. Pressure–temperature diagram of the experimental condition and phase equilibrium conditions of hydrates. Filled circle: CH_4 + THP hydrate [23]. Empty circle: CO_2 + THP hydrate [23]. Filled triangle: CH_4 simple hydrate [17]. Empty circle: CO_2 simple hydrate [17]. Cross: CO_2 simple hydrate [16]. Half rhombus: experimental condition in this study (CH_4 + CO_2 + THP system). Filled rhombus: CH_4 partial pressure of the experimental condition. Empty rhombus: CO_2 partial pressure of the experimental condition. The experimental condition of this study, p = 3.0 MPa and T = 285.1 K, was selected such that the CO_2 partial pressure falls outside of the CO_2 + THP hydrate stability region, while the CH_4 partial pressure is inside the CH_4 + THP hydrate stability region.

hydrate samples were conducted with the following procedures.

A fraction of crystal samples was placed in a high-pressure vessel with an inner volume of 150 cm^3. After evacuating the air inside the vessel quickly, the vessel was heated to 300 K to decompose all of the crystals. The composition of the gases was measured with gas chromatography.

PXRD measurement was performed for the rest of the crystal samples by parallel beam optics using Cu-Kα radiation (40 kV, 40 mA: model Ultima III, Rigaku Corp.) in the θ/2θ step scan mode with a step width of 0.02 degree at the temperature of 153 K. Crystalline structure and the hydrate lattice constant were analyzed using the RIETAN-FP program [33]. The hydrate-to-ice ratio of the sample was determined with the Rietveld analysis. The small cage occupancy of the gas molecules in the hydrate sample was estimated based on the masses of initially charged liquid samples (30.2 g of liquid water and 8.5 g of liquid THP), the measured gas consumption during the hydrate formation, the volume of

the gas phase after the hydrate formation considering the change in the total volume of condensed phases inside the reactor [34], and the hydrate-to-ice ratio.

2.3. Continuous CH_4/CO_2 separation

Continuous formation is a method of continuously producing a product by supplying all the necessary materials continuously in a mixing tank. A characteristic of the continuous formation process is that the conditions inside the mixing tank reach a steady state when operating the process. The apparatus for conducting continuous hydrate-based CH_4/CO_2 separation experiments in this study is depicted in Fig. 3. The hydrate-forming reactor with a couple of sight glass windows was made of stainless steel with a height of 210 mm, a diameter of 70 mm, and a total volume of 863 cm^3. By circulating an ethylene glycol solution as a coolant through the jacket covering the reactor, the temperature was controlled and measured with a Pt-resistance thermometer. The reactor was connected to a magnetic stirrer (model PSM-004C01F, Taiatsu Techno Co.) via a drive shaft. The shaft was equipped with six-blade impellers designed in a previous study [28] and a scraper for agitating the fluids in the reactor. Pressure in the reactor was measured using a pressure transducer (model PG-50KU, Kyowa Electric Instruments Co., Ltd.). The estimated measurement uncertainty of temperature was ±0.2 K. The estimated measurement uncertainty of the pressure was ±0.02 MPa. To prevent the backward feed gas flow, a check valve was placed between the feed gas cylinder and the reactor. Connected to the side wall of reactor was a plunger pump (model NP-LX-300, Nihon Seimitsu Kagaku Co., Ltd.) to supply liquid water and THP to the reactor. The time required to operate the plunger pump during the supply of the liquids was measured using a stopwatch (model SW-121 wt, Dretec Co., Ltd.). The vessels for sampling the gas phase and the hydrate slurry were connected to the bottom part of reactor. The vessel for gas sampling has an inner volume of 75 cm^3. The vessel for slurry sampling with an inner volume of 40 cm^3 (Vessel (1) in Fig. 3) was equipped with another same-size vessel (Vessel (2) in Fig. 3) for hydrate dissociation in the slurry and subsequently gas/liquid separation. The pressure of the gas dissociated from the slurry was measured with another pressure transducer (model PG-50KU). The mass of the sampled slurry was measured with an electronic balance (model UX420H, Shimadzu Corp.). It should be noted that the recovered THP and water from the obtained slurry can be reused in actual plant operations; THP is well-known to produce almost no peroxide after 30 days of air exposure 3536 and can thus be stably and safely reused for continuous hydrate formation. Moreover, the long-term stability of the thermophysical properties of hydrate has been experimentally demonstrated by Yamamoto et al. [37] through the 200 cycles of hydrate formation and dissociation. The compositions of the gas phase and the gaseous components obtained from the sampled hydrate slurry were analyzed using a gas chromatograph (model GC 3210, GL Sciences Inc.). The analytical standard deviation for gas chromatography was determined to be 0.001 in mole fraction by more than five-time injections of the same mixed $CH_4 + CO_2$ mixed gas sample, which was used as the uncertainty of the measurement. For the evacuation of the entire apparatus, a vacuum pump was attached.

The flow diagram for the operation of continuous hydrate-based CH_4/CO_2 separation is shown in Fig. 4. Before the experiment, the air

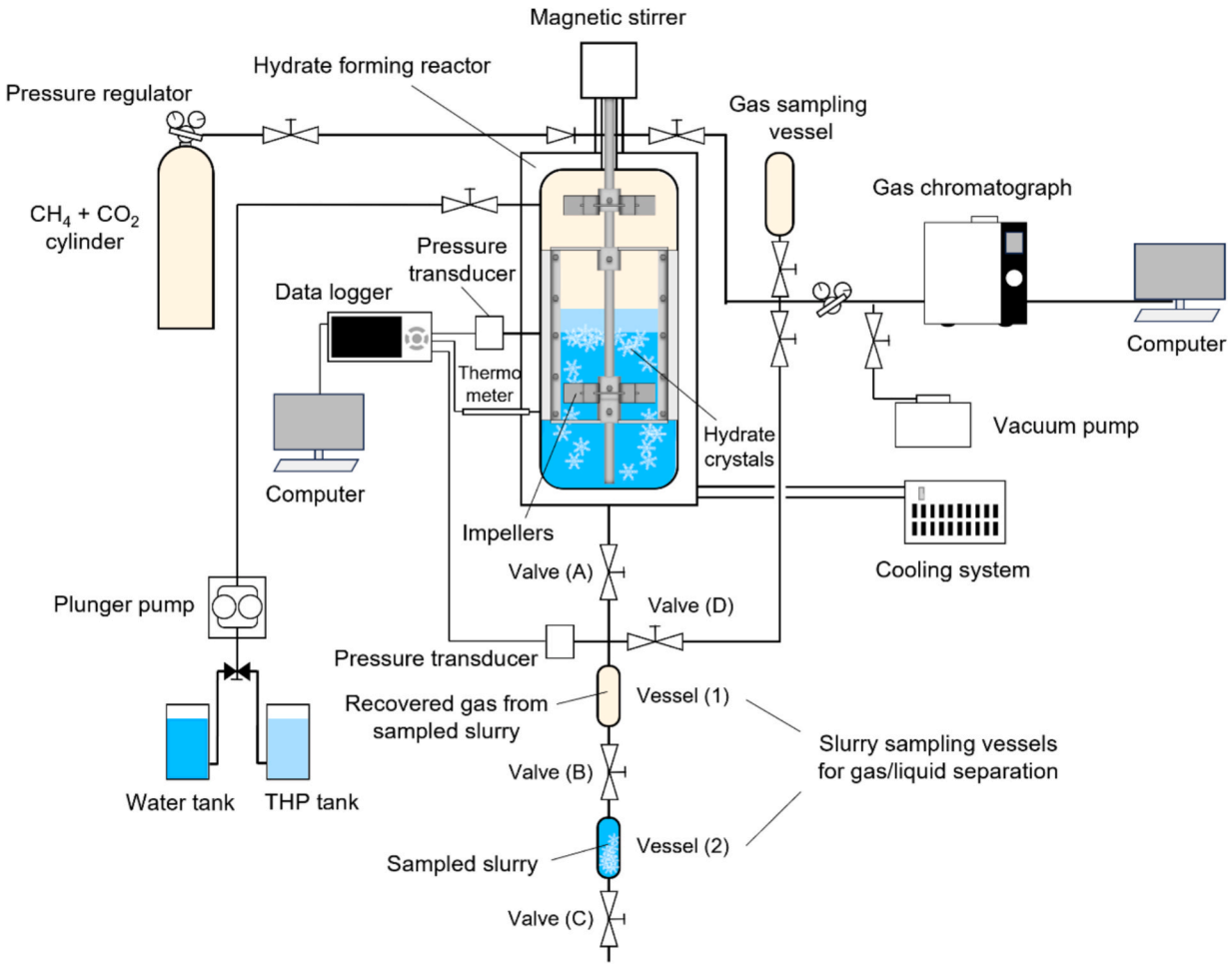

Fig. 3. Layout of the apparatus for continuous hydrate-based CH_4/CO_2 separation experiment.

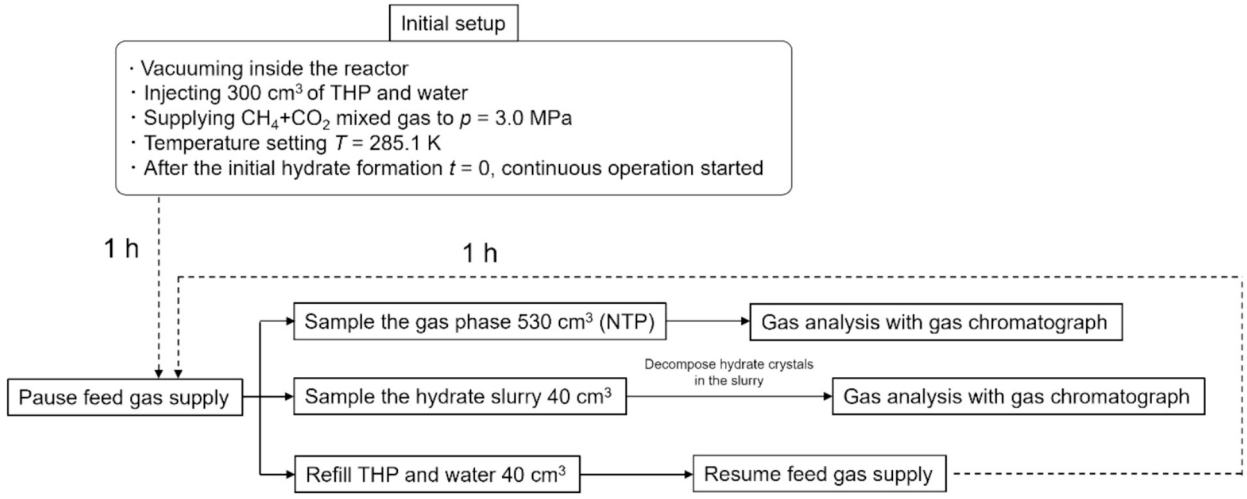

Fig. 4. Schematic block flow diagram of the continuous hydrate-based CH_4/CO_2 separation.

inside the reactor was evacuated. The first step of the process was the injection of 300 cm^3 of THP + water mixture. The mass fraction of THP in the mixture, w_{THP}, was set to $w_{THP} = 0.11$ or $w_{THP} = 0.055$. These fractions were set as the half portion of $w_{THP} = 0.22$, which corresponds to the stoichiometric composition of the structure II hydrate, or a quarter of that portion. $CH_4 + CO_2$ gas mixture was then supplied to 3.0 MPa to the reactor. The reactor was cooled to 285.1 K. Agitation in the reactor with the magnetic stirrer was initiated at 400 rpm or 80 rpm, the rate set by trial and errors. Once the initial hydrate formation was observed visually ($t = 0$), the continuous operation every hour was started. The feed gas supply was paused temporarily for the moment of sampling procedure. Approximately 530 cm^3 (NTP) from the gas phase and 40 cm^3 of the hydrate slurry were sampled from the reactor. Sampling of hydrate slurry was conducted in the vessel (1) in Fig. 3 by opening the valve (A) while closing the valves (B), (C), and (D). The sampled slurry was transported to vessel (2) by opening the valve (B), where the hydrate was decomposed at 298 K for 40 min and subsequently the recovered gas was separately collected in the upper vessel (1). The remaining liquid THP + water mixture obtained from the sampled slurry was discharged. The mass and the temperature of the remaining liquid collected in the vessel (2) were measured. The gas compositions in both of the sampling vessels were analyzed using a gas chromatograph and hourly recorded. The equivalent amount of liquid water and THP was refilled to the reactor to maintain the prescribed w_{THP} inside the reactor. Through the entire experiment, the discharge flow rate of the plunger pump was fixed at 600 mL/min, namely 10 mL/s. By measuring the time required to operate the plunger pump, the supply volume of the liquid sample was adjusted. For example, when refilling a 29.6 g of THP + water mixture (26.3 g of water and 3.3 g of THP), the plunger pump was operated for 2.6 s to supply the water, followed by 0.4 s to supply the THP. After refilling the THP and water in this manner, we confirmed that the system pressure was unchanged before the discharge of hydrate slurry, meaning that an equal volume of liquid had been resupplied. Immediately afterwards within a few seconds, the feed gas supply was resumed. The above procedure was repeated for over 24 h until the compositions of both phases reached a steady state.

3. Results and discussion

3.1. Semi-batch CH_4/CO_2 separation with PXRD analysis

Hydrate-based semi-batch CH_4/CO_2 separation experiment was performed in $CH_4 + CO_2$ + THP + water system to evaluate the concentration of CH_4 in the hydrate phase formed with intermittently supplied $CH_4 + CO_2$ gas mixture. The CH_4: CO_2 composition in the gas phase before hydrate formation and the composition in the hydrate phase after hydrate formation were quantified with gas chromatography. The result of the measurement is summarized in Table 1. As shown in Table 1, the initial composition of the feed gas was CH_4: CO_2 = 0.600: 0.400. After the hydrate formation in semi-batch reactor, the composition in the hydrate phase reached CH_4: CO_2 = 0.811: 0.189. The mole fraction of CH_4 increased from 0.600 to 0.811, demonstrating that CH_4 was preferably captured and therefore concentrated in the hydrate phase. The measured gas consumption during the entire semi-batch hydrate formation was 2.4 L at 0.1 MPa, 285.1 K. This volume of the gas consumption indicates the amount of gas incorporated in the hydrate. This value is approximately more than 100 times larger than the amount of gases dissolved in water; the calculated amount of CO_2 and CH_4 dissolved in 30.2 g of water are 2.48×10^{-2} L and 1.02×10^{-3} L, respectively. Thus, the higher solubility of CO_2 compared to CH_4 in water has no more than 1 % effect on the preferential capture of CH_4 by hydrate formation. The result revealed that hydrate-based CH_4 enrichment in $CH_4 + CO_2$ gas mixture can be achieved in $CH_4 + CO_2$ + THP + water system.

For the semi-batch operation, there are previous investigations to quantify the time-resolved gas uptake during the hydrate formation [38–40]. Only a few experimental techniques, such as Raman spectroscopy, can determine the time-resolved compositions of the gas and hydrate phases during hydrate formation [41,42].

The PXRD profiles of hydrate in the same semi-batch hydrate formation method in $CH_4 + CO_2$ + THP + water system measured at 153 K are presented in Fig. 5. All of the diffraction patterns and the peak positions presented in Fig. 5 was obtained with the calculation from the Rietveld analysis. The assignment of the PXRD patterns shown in Fig. 5 indicated that the crystalline structure of the hydrate formed with CH_4, CO_2, and THP is structure II. The lattice constant determined by the PXRD analysis was 1.73064(5) nm. This lattice constant of $CH_4 + CO_2$ + THP hydrate lies between the values of lattice constant of CH_4 + THP hydrate and CO_2 + THP hydrate, which were reported to be 1.72998 nm and 1.73300 nm, respectively, at 153 K [43]. A slight expansion of the lattice of $CH_4 + CO_2$ + THP hydrate compared to CH_4 + THP hydrate would be induced by the partial occupation of CO_2 in the hydrate

Table 1
CH_4: CO_2 composition before and after hydrate-based semi-batch separation.

	Mole fraction before the hydrate formation	Mole fraction after the hydrate formation
CH_4	0.600	0.811
CO_2	0.400	0.189

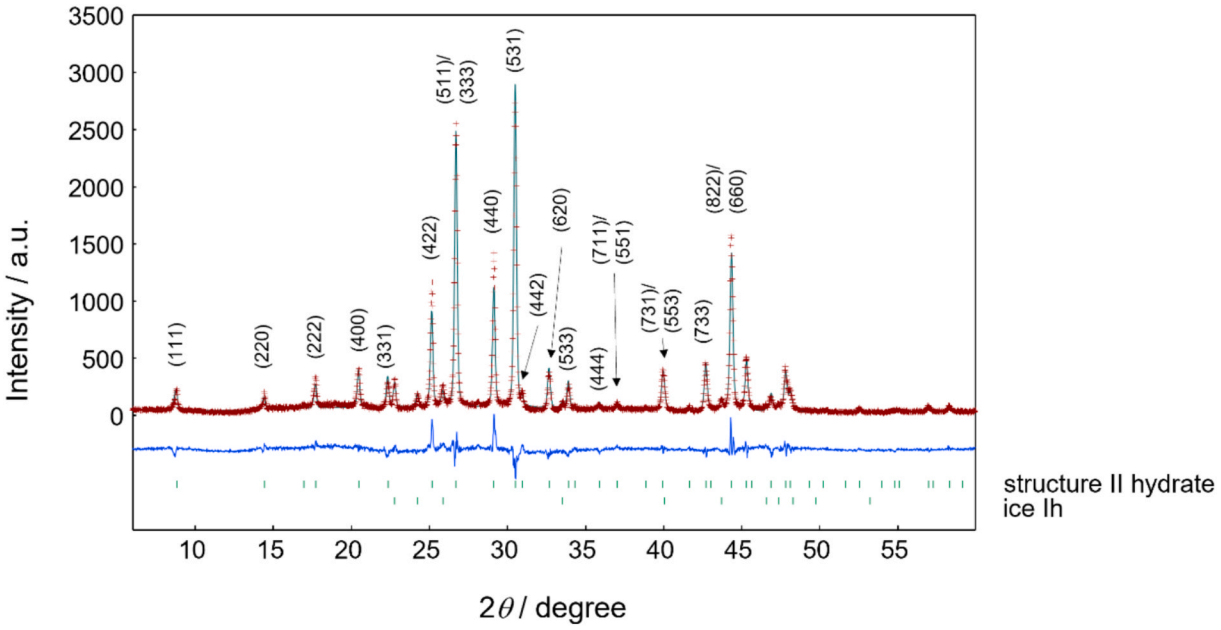

Fig. 5. Powder X-ray diffraction pattern of hydrate formed in the system of CH_4 + CO_2 + THP + water. The measurement was performed at 153 K. The lattice constant of hydrate was determined to be 1.73064(5) nm. The red tick marks and the black line in the upper part indicate the diffracted pattern and calculated pattern from the Rietveld analysis. The blue line is a deviation between the diffracted and calculated patterns. The green tick marks denote the peak positions obtained with the calculation from the Rietveld analysis for structure II hydrate and hexagonal ice (Ih), respectively. The figure also shows the Miller indices for sII hydrates with 2θ angles of 45 degrees or less. (For interpretation of the references to colour in this figure legend, the reader is referred to the web version of this article.)

structure. The hydrate-to-ice ratio of the sample was determined to be structure II hydrate: ice Ih = 0.96: 0.04 with the Rietveld analysis. The small cage occupancy of CH_4 and CO_2 in total in the formed structure II hydrate was estimated to be 58 %, based on the above determined water-to-hydrate conversion ratio (96 %), masses of charged liquids, the measured gas consumption, and the estimated gas phase volume after the hydrate formation.

Udachin et al. [44] performed single XRD analysis on THP simple hydrate and suggested the presence of guest–host hydrogen bonding by determining the distance between the O atoms of THP and cage water molecules. Iino et al. [23] characterized CO_2 + THP hydrate and CH_4 + THP hydrate using PXRD. They reported that the small cage occupancy of CH_4 in the CH_4 + THP hydrate (above 98 %) was higher than that of CO_2 in the CO_2 + THP hydrate (59 %). Based on the above studies, Narayanan et al. [43] investigated these binary guest hydrates using molecular dynamics simulations and PXRD. They observed that the lattice of the CO_2 + THP hydrate expanded compared to that of the CH_4 + THP hydrate. This expansion could be attributed to the asymmetry of the CO_2 molecule, which could distort the small cages of structure II hydrate and hinder the encasement of CO_2 within the small cages.

The results have proved that CH_4 was enriched in the structure II hydrate phase in CH_4 + CO_2 + THP + water system. The CH_4 selectivity in CH_4 + CO_2 gas mixture of THP as an structure II-hydrate-forming guest compound was proved to be comparably high to other structure II-forming compounds tested in a previous study by Seo et al. [25]; their batch experiment in the systems with *tert*-butyl alcohol or trimethylene oxide showed that the CH_4 obtained from the structure II hydrate phase increased from 0.600 to 0.701 or 0.746 in mole fraction. The semi-batch results of this study, therefore, implied that the semi-batch operation enables more effective conversion of water to hydrate compared to the batch operation. As mentioned above, the hydrate-to-ice ratio of the above semi-batch sample was determined to be structure II hydrate: ice Ih = 0.96: 0.04 with the Rietveld analysis. On the other hand, based on the gas uptake data for hydrate-based batch separation study by Seo et al. [25], the water-to-hydrate molar conversion is estimated to be maximal 77 %. Therefore, the semi-batch operation could exhibit a higher water-to-hydrate conversion than the batch operation. Consequently, the higher water-to-hydrate conversion for the semi-batch operation could contribute to the higher CH_4 selectivity compared to the batch operation.

3.2. *Continuous CH_4/CO_2 separation*

Continuous hydrate-based CH_4/CO_2 separation experiment was conducted in CH_4 + CO_2 + THP + water system at first with the THP mass fraction w_{THP} = 0.11 under the stirring rate of 400 rpm. Temperature and pressure conditions were 285.1 K and 3.0 MPa, respectively. The THP mass fraction was set to the half portion of the stoichiometric composition of the structure II hydrate, w_{THP} = 0.22. Previous THP-hydrate-based continuous formation experiments revealed that with w_{THP} = 0.22, the THP mass fraction would be too high and caused clogging of reactor with hydrate crystals. In contrast, when w_{THP} = 0.11 was chosen, the fluidity of the hydrate slurry can be maintained within the entire process of continuous operation 15,28. However, the experimental trial in this study, with w_{THP} = 0.11 at 400 rpm, failed after t = 3h. The failure in continuous operation was detected by measuring the mass of sampled slurry, which is presented in Fig. 6. As shown in Fig. 6, from t = 0 to t = 3h, the mass of sampled slurry decreased from around 40 g to 0 g. This mass drop in sampled slurry was likely caused by the stacked hydrate accumulation on the walls and the bottom of reactor, preventing the discharge of liquid when sampling. The photographs inside the reactor during the experiment for each condition are shown in Fig. 7(a). The mechanism for clogging hydrate was illustrated in Fig. 7 (b). Once the hydrate accumulation happens, the continuation of the continuous separation process turns into an impossible task. To solve the above problem, either the stirring rate or the THP mass fraction should be reduced to control the solid fraction of the slurry and maintain the fluidity of slurry. Therefore, another experimental run in CH_4 + CO_2 + THP + water system with w_{THP} = 0.11 at a reduced stirring rate of 80 rpm was conducted. The reduction of the stirring rate should result in the reduction of sites of hydrate nucleation and growth in the reactor, thereby contributing to the control of solid fraction of the slurry.

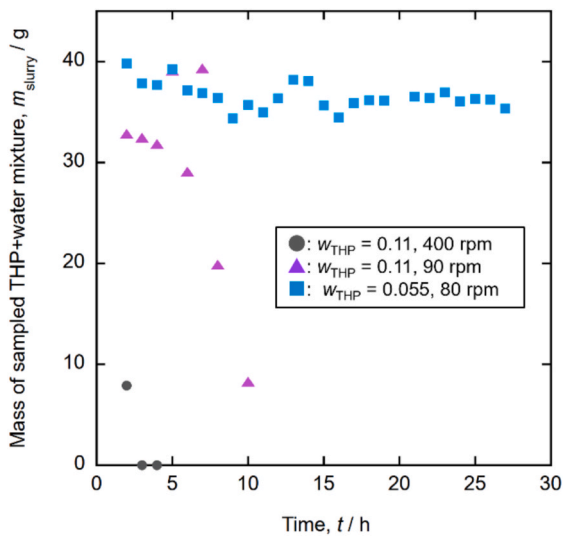

Fig. 6. Time evolution of the mass of sampled liquid (mixture of THP and water) recovered from the hydrate slurry during the continuous hydrate-based CH_4/CO_2 separation in the $CH_4 + CO_2 + THP + water$ system at $T = 285.1$ K, $p = 3.0$ MPa. ●: $w_{THP} = 0.11$ at 400 rpm; ▲: $w_{THP} = 0.11$ at 90 rpm; ■: $w_{THP} = 0.055$ at 80 rpm.

Nevertheless, the experimental trial with these conditions also failed at $t = 7$h in the same way. The reason why the accumulation of hydrate tended to occur in this $CH_4 + CO_2 + THP + water$ system could be that the driving force for the hydrate formation was maintained during the continuous formation process. Previous continuous formation experiments mentioned above 15,28 employed $H_2 + CO_2$ gas mixture or $N_2 + CO_2$ gas mixture as feed gas. In these systems for CO_2 capture, the partial pressure of CO_2 decreased over the continuous hydrate formation process, thereby reducing the driving force and causing the hydrate accumulation less likely to occur. By contrast, this study employed $CH_4 + CO_2$ gas mixture as feed gas. The use of different feed gases should affect the driving force, which in turn has an influence on the possibility of hydrate accumulation. To further improve the conditions enabling stable continuous operation, another experimental run with $w_{THP} = 0.055$ at 80 rpm was tested.

The continuous hydrate-based CH_4/CO_2 separation experiment was performed in $CH_4 + CO_2 + THP + water$ system with the THP mass fraction $w_{THP} = 0.055$ at 80 rpm. The experimental temperature and pressure conditions set through the entire experiment were 285.1 K and 3.0 MPa, respectively. Under these conditions, hydrate-based continuous operation with the feed $CH_4 + CO_2$ gas mixture (CH_4: $CO_2 = 0.60$: 0.40) succeeded with the changing compositions of gas and slurry phases reached a steady state after over 24 h. The stirring power/volumetric energy consumption (P/V) was estimated to be 133 kW/m^3 in this system, based on the stirring power with the used magnetic stirrer of 40 W. The time evolutions of recorded compositions for the gas phase and for the hydrate slurry during the measurement are presented in Figs. 8 and 9, respectively. While multiple trials were conducted for each experimental condition, the technical challenges with continuous separation resulted in an error in data acquisition or recording on some sets of trials. Consistent hourly data recording on CH_4: CO_2 mole fraction was not always successful across all trials. Therefore, we showed a set of complete and representative hourly-recorded data sample for each experimental condition in the figures. Both figures describe the correlation between the elapsed time, t, and $x_{i,gas}$ or $x_{i,slurry}$. $x_{i,gas}$ indicates the recorded mole fraction of gaseous component i (CH_4 or CO_2) in the gas phase, whereas $x_{i,slurry}$ denotes the recorded mole fraction of the component recovered from the hydrate slurry. As shown in Fig. 8, in the first hour $t = 1$h, $x_{CH4,gas}$ had increased from the initial composition 0.60 to 0.61, where $x_{CO2,gas}$ decreased from the initial composition 0.40 to 0.39. This increase in $x_{CH4,gas}$ from the feed gas composition could be caused by the preferable dissolution of CO_2 into the liquid phase. With the time proceeded from $t = 1$h to $t = 25$ h, $x_{CH4,gas}$ has then gradually decreased from 0.61 to 0.58, while $x_{CO2,gas}$ has increased from 0.39 to 0.42. After $t = 25$ h, the mole fractions reached a steady state, with $x_{CH4,gas}$ being 0.58 and $x_{CO2,gas}$ being 0.42. The continuation of hydrate-forming operation and the steady state for three more hours until $t = 27$ h was experimentally confirmed. This result suggests that CH_4 is preferentially captured in the hydrate structure, while CO_2 is enriched in the gas phase through the continuous separation process.

The time evolution of CH_4 and CO_2 mole fractions recovered from

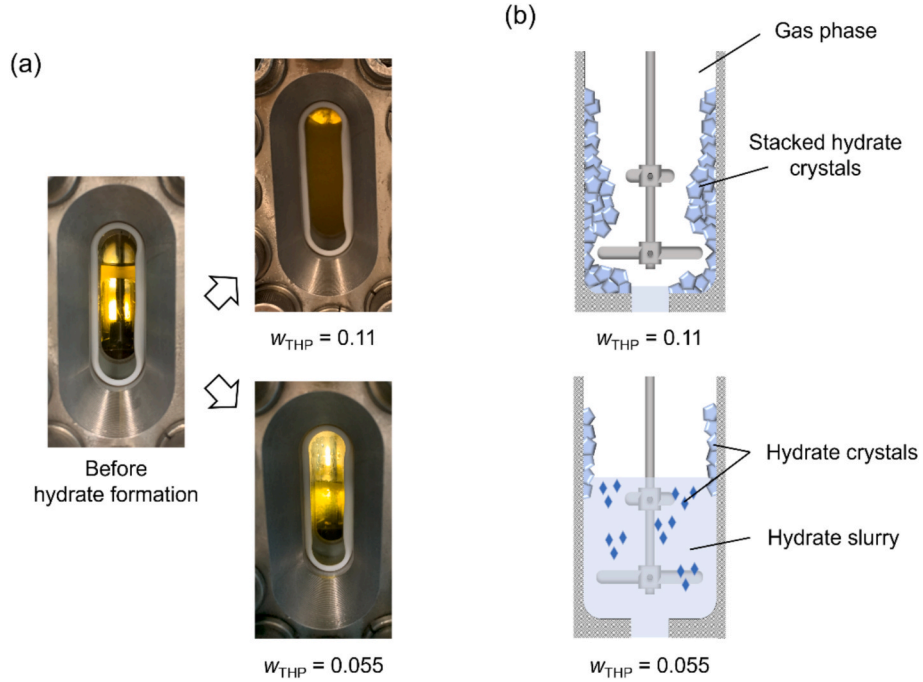

Fig. 7. (a) Photographs and (b) illustration inside the reactor describing hydrate accumulation on the wall during the trial of hydrate continuous formation.

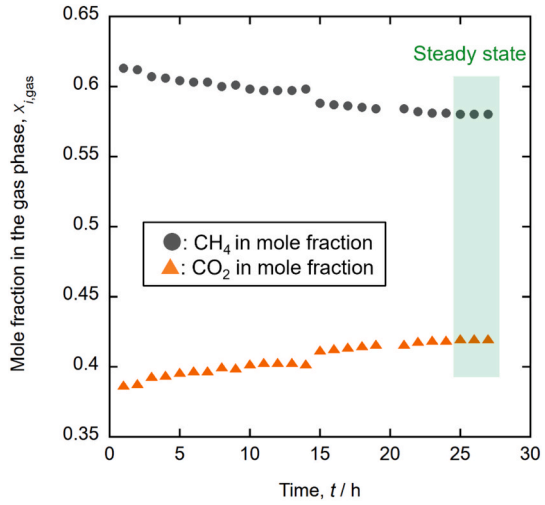

Fig. 8. Time evolution of the recorded compositions of the gas phase for continuous hydrate-based CH_4/CO_2 separation in the CH_4 + CO_2 + THP + water system at T = 285.1 K, p = 3.0 MPa, w_{THP} = 0.055 at 80 rpm. The subscript i denotes CH_4 or CO_2. ●: Mole fraction of CH_4; ▲: Mole fraction of CO_2. The estimated uncertainty of measurement was 0.001 in mole fraction.

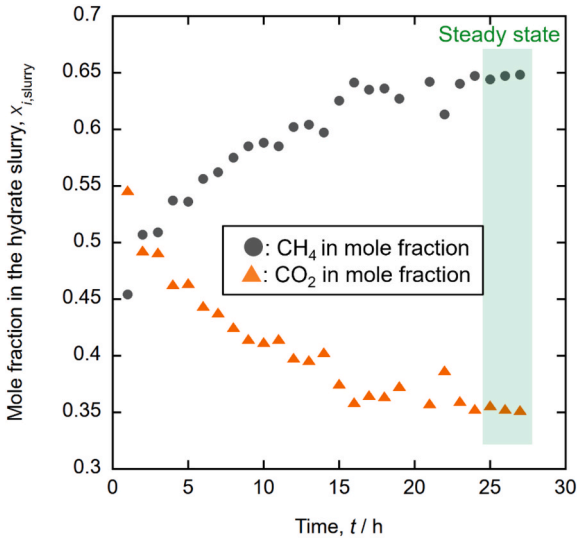

Fig. 9. Time evolution of the recorded compositions of the hydrate slurry for continuous hydrate-based CH_4/CO_2 separation in the CH_4 + CO_2 + THP + water system at T = 285.1 K, p = 3.0 MPa, w_{THP} = 0.055 at 80 rpm. The subscript i denotes CH_4 or CO_2. ●: Mole fraction of CH_4; ▲: Mole fraction of CO_2. The estimated uncertainty of measurement was 0.001 in mole fraction.

the hydrate slurry is presented in Fig. 9. As shown in Fig. 9, the $x_{CH4,slurry}$ was 0.45 at t = 1h, gradually increased with time, and reached 0.65 at t = 24 h. This result demonstrates that the continuous hydrate-based CH_4 enrichment from the CH_4 + CO_2 gas mixture using THP has succeeded. The composition changed from CH_4: CO_2 = 0.60: 0.40 as the feed gas to CH_4: CO_2 = 0.65: 0.35 in the hydrate slurry phase after reaching the steady state in continuous operation.

Fig. 10(a) presents the time evolution of the measured pressure of the gas recovered from the slurry. The slurry was heated at T = 296.6 K in the Vessel (1) with an inner volume of 40 cm^3, which is depicted in Fig. 3. Fig. 10(b) shows the temporal evolution of the hydrate volume fraction in the slurry, Φ_h, estimated based on the measured pressure depicted in Fig. 10(a), the mass of sampled liquid presented in Fig. 6, and the small cage occupancy of hydrate (58 %) determined in the Section 3.1. As shown in Fig. 10(a), the pressure of recovered gas from the sampled hydrate slurry was around 1 MPa in the first few hours and increased with time. Reaching the steady state after t = 25 h, the pressure reached 3.7 MPa. As shown in Fig. 10(b), Φ_h was around 0.1 in the first few hours. Φ_h also increased with time and reached 0.43 at the steady state after t = 25 h. Controlling the solid fraction of the slurry is critical for ensuring the transportation from the reactor in continuous processes. When the solid fraction is too high, slurry may adhere to the vessel walls, potentially causing clogging [45]. The hydrate volume fraction obtained in this experiment, Φ_h = 0.43, may represent the critical volume fraction (Φ_{crit}).

During the continuous CH_4 separation process, $x_{CH4,slurry}$ increased from 0.45 to 0.65 until reaching the steady state. This could be attributed to the increase in the amount of CH_4 in the sampled hydrate slurry as time proceeded. The CH_4 uptake into the hydrate per unit mass $\xi_{CH4,slurry}$ can be calculated as follows:

$$\xi CH4, slurry = \frac{n_{CH_4,slurry}}{m_{slurry}} \quad (1)$$

where $n_{CH4,slurry}$ denotes the amount of the captured CH_4, which was calculated from the measured pressure, temperature and mole fraction in the dissociated hydrate slurry. m_{slurry} stands for the mass of measured sampled slurry. The time evolution of the CH_4 uptake during the continuous separation process is described in Fig. 11. As shown in Fig. 11, $\xi_{CH4,slurry}$ at t = 1h was 0.7 mol/kg. As time proceeded, $\xi_{CH4,slurry}$ increased from t = 1h to t = 15 h to reach 2.0 mol/kg. The value of $\xi_{CH4,slurry}$ was maintained around 2.0 mol/kg after t = 15 h and reaching the steady state. This tendency could be caused by the increase in the amount of formed hydrate in the reactor; at the start of the continuous hydrate formation process, the formed amount of hydrate would be little, or the CH_4 concentration in the hydrate phase would be lower. The amount could be increased over time during the continuous hydrate formation process. This increasing tendency implied that the driving force for hydrate formation was maintained over the entire process in this CH_4 + CO_2 system, as mentioned above in the first paragraph.

The obtained results of this study clearly revealed that CH_4 is enriched in structure II hydrate in CH_4 + CO_2 + THP + water system both with semi-batch and continuous operations. The result demonstrates a trend in hydrate-based gas capture from CH_4 + CO_2 gas mixture opposite to that of the previous study using structure I hydrate; Tomita et al. [19] performed continuous hydrate-based separation experiments in CH_4 + CO_2 + water system, showing that CO_2 is concentrated in the structure I hydrate slurry. Against the fact that hydrate formation from CH_4 + CO_2 gas mixture induces structure I CO_2-rich hydrate, the results of this study presented that the addition of THP as a large molecule guest compound (LMGC) for continuous hydrate formation promotes structure II CH_4-rich hydrate. The continuous CH_4/CO_2 separation experiments in this study showed that CH_4-rich hydrate can be formed continuously during long-term operations. The obtained time-dependent tendency of the compositional changes in hydrate indicated that the CH_4 enrichment in the structure II-hydrate slurry tested in this study is similarly efficient compared to the CO_2 enrichment in the structure I-hydrate slurry by Tomita et al. [19]; in both of the measurements, compositions of the targeted gas (CH_4 or CO_2) in the hydrate slurry have increased in approximately 20 %. These insights will enhance the development of biogas separation technology which could stabilize CH_4 into hydrate slurry.

Table 2 summarizes the experimental achievement of structure II-hydrate-based CH_4 enrichment from CH_4 + CO_2 gas mixture. By looking at the individual compositional change indicated in Table 2, the separation performance of the continuous separation process is lower compared to the batch and semi-batch separation processes. As determined in the Section 3.1, the hydrate solid fraction of the semi-batch sample was 0.96. For the continuous process, the hydrate solid fraction in the slurry was estimated to be 0.43 at the steady state, as depicted in Fig. 10(b). Therefore, the semi-batch operation could exhibit a higher

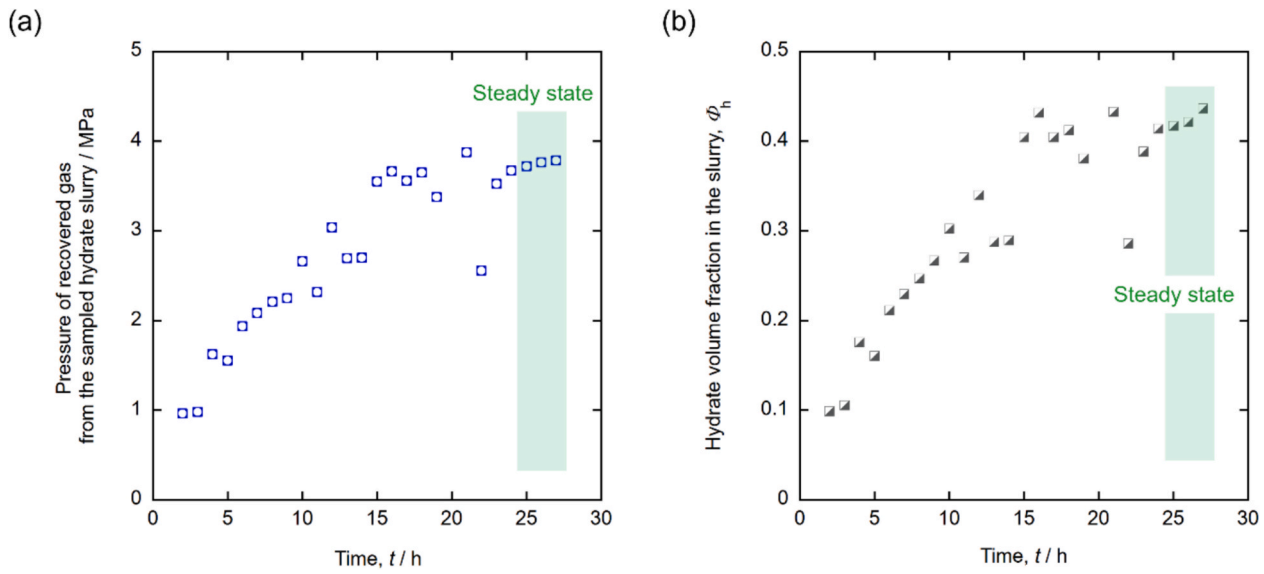

Fig. 10. (a) Time evolution of the pressure of the gas recovered from the sampled slurry for continuous hydrate-based CH_4/CO_2 separation in the $CH_4 + CO_2 + THP + water$ system at $T = 285.1$ K, $p = 3.0$ MPa, $w_{THP} = 0.055$ at 80 rpm. (b) Time evolution of the estimated hydrate volume fraction in the slurry, Φ_h, for continuous hydrate-based CH_4/CO_2 separation in the $CH_4 + CO_2 + THP + water$ system at $T = 285.1$ K, $p = 3.0$ MPa, $w_{THP} = 0.055$ at 80 rpm.

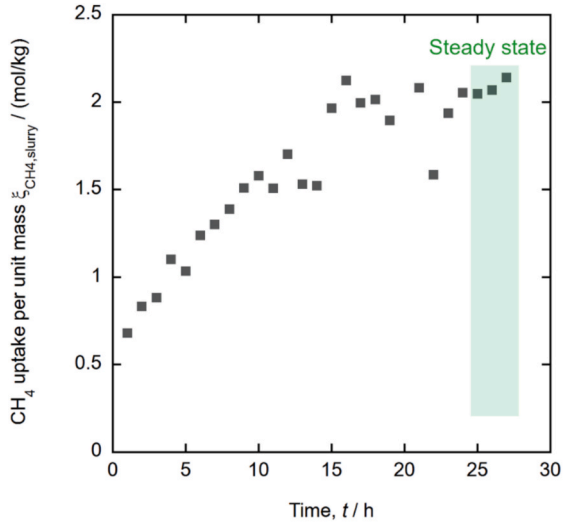

Fig. 11. Time evolution of the CH_4 uptake into the hydrate slurry per unit mass $\xi_{CH4,\ slurry}$ for continuous hydrate-based CH_4/CO_2 separation in the $CH_4 + CO_2 + THP + water$ system at $T = 285.1$ K, $p = 3.0$ MPa, $w_{THP} = 0.055$ at 80 rpm. The estimated uncertainty of measurement was 0.02 mol/kg.

Table 2
Experimental results of structure II-hydrate-based CH_4 enrichment from $CH_4 + CO_2$ gas mixture.

Method of gas separation	Feed gas composition by mole fraction	Composition after hydrate formation	Separation factor α
Batch process (Seo et al. [25])	CH_4: CO_2 = 0.61: 0.39	CH_4: CO_2 = 0.74: 0.26	1.82
Semi-batch process (this study)	CH_4: CO_2 = 0.60: 0.40	CH_4: CO_2 = 0.81: 0.19	2.84
Continuous process (this study)	CH_4: CO_2 = 0.60: 0.40	CH_4: CO_2 = 0.65: 0.35	1.24

water-to-hydrate conversion within a single reactor than the continuous operation. Consequently, the higher water-to-hydrate conversion for the semi-batch operation could contribute to the higher CH_4 selectivity compared to the continuous operation.

Nevertheless, it is essential to understand the properties related to the continuous process to scale up and to implement the hydrate-based biogas separation plants. In general, the design of large-scale plants is predicated on continuous operation. The detailed engineering designs of scaled-up continuous hydrate formation processes with water inlet flow rates of 1 to 82 tons per hour have been provided in previous publications [46–49]. This is because the process design and operation can be greatly simplified by introducing the continuous formation system; both the batch and semi-batch system can only treat the limited volume of gas per single reactor and would therefore require numerous sets of reactors for large-scale operation. On the other hand, for continuous operation, only a single reactor unit would suffice for each gas separation step. Aiming at large-scale operations, a practical reactor design with a tubular reactor utilizing two phase flow composed of continuous liquid water and dispersed guest gas phases has been experimentally investigated [47,48]. The introduction of two-phase flow reactors may enhance the removal of hydrate formation heat and the mixing of water and the guest compounds for improved kinetics. The practical advantage and industrial relevance thus lie in terms of technical and economic perspectives.

4. Conclusions

In the present study, CH_4/CO_2 gas separation experiments using the formation of hydrate in $CH_4 + CO_2 + THP + water$ system were performed with semi-batch and continuous separation methods aimed at biogas separation. For both types of experiment, measurements were conducted at 285.1 K and 3.0 MPa. Results obtained from the semi-batch experiment revealed that CH_4 is concentrated in the hydrate phase from CH_4: CO_2 = 0.60: 0.40 to CH_4: CO_2 = 0.81: 0.19. The crystalline structure of the $CH_4 + CO_2 + THP$ hydrate was identified structure II by employing the PXRD analysis. The results suggested that THP can support the capture of CH_4 via structure II hydrate formation. Continuous separation experiment for over 27 h in $CH_4 + CO_2 + THP + water$ system demonstrated that the composition in the hydrate slurry reached CH_4: CO_2 = 0.65: 0.35 at the steady state, where the continuous CH_4 enrichment in the hydrate has succeeded. In the continuous separation

experiment of this study, a slurry with a hydrate volume fraction (Φ_h) of 0.43 was successfully discharged from the reactor without clogging to the reactor walls, which may represent the critical volume fraction (Φ_{crit}). The overall results presented in this study showed that structure II hydrate is a promising material for CH_4 capture in biogas not only in terms of batch-type operation as indicated in previous studies but also with semi-batch as well as the continuous separation methods, both of which being preferable for engineering practice.

CRediT authorship contribution statement

Meku Maruyama: Writing – original draft, Visualization, Validation, Methodology, Investigation, Funding acquisition, Formal analysis, Data curation, Conceptualization. **Satoshi Takeya:** Writing – review & editing, Validation, Resources, Methodology, Investigation. **Judith M. Schicks:** Writing – review & editing, Conceptualization. **Ryo Ohmura:** Writing – review & editing, Validation, Resources, Funding acquisition, Conceptualization.

Declaration of competing interest

The authors declare that they have no known competing financial interests or personal relationships that could have appeared to influence the work reported in this paper.

Acknowledgements

This study was supported by a Grant-in-Aid for JSPS Fellows from the Japan Society for the Promotion of Science [Grant Number JP23KJ1911] and a Keirin-racing-based research promotion fund from the JKA Foundation (Grant Number 2022M-270). M.M. would like to thank Tomoaki Ishikawa for his insightful experimental advice and support. Additionally, the assistance of Ryonosuke Kasai in estimating power consumption of the magnetic stirrer is gratefully acknowledged.

Data availability

All data are included in supplementary files and are available through Zenodo at https://doi.org/10.5281/zenodo.18057344.

References

[1] United Nations, Paris Agreement. https://unfccc.int/sites/default/files/english_paris_agreement.pdf, Paris, 12.12.2015 (accessed 20 August 2025).
[2] European Commission, A Clean Planet for all - A European strategic long-term vision for a prosperous, modern, competitive and climate neutral economy. https://eur-lex.europa.eu/legal-content/EN/TXT/?uri=CELEX:52018DC0773, Brussels, 28.11.2018 (accessed 07 May 2025).
[3] Ryckebosch E, Drouillon M, Vervaeren H. Techniques for transformation of biogas to biomethane. Biomass Bioenergy 2011;35:1633–45. https://doi.org/10.1016/j.biombioe.2011.02.033.
[4] Das K, Kumar S, Bhattacharya S. Biomass gasification in an industrial-scale entrained flow gasifier and effects of various parameters on gasification performance: an approach based on numerical models. Fuel 2026;405:136537. https://doi.org/10.1016/j.fuel.2025.136537.
[5] Varthan MKH, Keerthana V, Saravanan A, Deivayanai VC, Kumar RSR, Raveendran SK, et al. Harnessing global biomass for bioenergy: assessment techniques, technological advances, and environmental perspectives. Fuel 2026;405:136599. https://doi.org/10.1016/j.fuel.2025.136599.
[6] Rasi S, Veijanen A, Rintala J. Trace compounds of biogas from different biogas production plants. Energy 2007;32:1275–380. https://doi.org/10.1016/j.energy.2006.10.018.
[7] Rasi S, Lehtinen J, Rintala J. Determination of organic silicon compounds in biogas from wastewater treatments plants, landfills, and co-digestion plants. Renew Energy 2011;35:2666–73. https://doi.org/10.1016/j.renene.2010.04.012.
[8] Salazar Gomez JI, Lohmann H, Krassowski J. Determination of volatile organic compounds from biowaste and co-fermentation biogas plants by single-sorbent adsorption. Chemosphere 2016;153:48–57. https://doi.org/10.1016/j.chemosphere.2016.02.128.
[9] Calbry-Muzyka A, Madi H, Rüsch-Pfund F, Gandiglio M, Biollaz S. Biogas composition from agricultural sources and organic fraction of municipal solid waste. Renew Energy 2022;181:1000–7. https://doi.org/10.1016/j.renene.2021.09.100.
[10] Augelletti R, Conti M, Annesini MC. Pressure swing adsorption for biogas upgrading. a new process configuration for the separation of biomethane and carbon dioxide. J Clean Prod 2017;140:1390–8. https://doi.org/10.1016/j.jclepro.2016.10.013.
[11] Abd AA, Othman MR. Biogas upgrading to fuel grade methane using pressure swing adsorption: parametric sensitivity analysis on an industrial scale. Fuel 2022;308:121986. https://doi.org/10.1016/j.fuel.2021.121986.
[12] Abd AA, Othman MR, Majdi HS, Helwani Z, Shamsudin IK. Evaluation of ZIF-7 media for biogas upgrading into vehicular fuel quality standard by pressure swing adsorption through experiment and dynamic simulation under non-isothermal conditions. Fuel 2023;350:128863. https://doi.org/10.1016/j.fuel.2023.128863.
[13] Kumari A, Kaushik K, Shankar A, Aneja R, Chauhan A, Saini VK. Influence of hierarchical porosity on the adsorption selectivity of activated carbons prepared via different activation methods for biogas upgradation. Fuel 2025;399:135651. https://doi.org/10.1016/j.fuel.2025.135651.
[14] Vu HP, Nguyen LN, Wang Q, Ngo HH, Liu Q, Zhang X, et al. Hydrogen sulphide management in anaerobic digestion: a critical review on input control, process regulation, and post-treatment. Bioresour Technol 2022;346:126634. https://doi.org/10.1016/j.biortech.2021.126634.
[15] Kiyokawa H, Horii S, Alavi S, Ohmura R. Improvement of continuous hydrate-based CO_2 separation by forming structure II hydrate in the system of $H_2 + CO_2 + H_2O$ + Tetrahydropyran (THP). Fuel 2020;278:118330. https://doi.org/10.1016/j.fuel.2020.118330.
[16] Ito H, Gibo A, Shiraishi S, Yasuda K, Ohmura R. Renewed measurements of carbon dioxide hydrate phase equilibrium. Int J Thermophys 2023;44:128. https://doi.org/10.1007/s10765-023-03241-y.
[17] Adisasmito S, Frank III RJ, Sloan Jr ED. Hydrates of carbon dioxide and methane mixtures. J Chem Eng Data 1991;36:68–71. https://doi.org/10.1021/je00001a020.
[18] van Denderen M, Ineke E, Golombok M. CO_2 removal from contaminated natural gas mixtures by hydrate formation. Ind Eng Chem Res 2009;48:5802–7. https://doi.org/10.1021/ie8017065.
[19] Tomita S, Akatsu S, Ohmura R. Experiments and thermodynamic simulations for continuous separation of CO_2 from $CH_4 + CO_2$ gas mixture utilizing hydrate formation. Appl Energy 2015;146:104–10. https://doi.org/10.1016/j.apenergy.2015.01.088.
[20] Wang F, Fu S, Guo G, Jia Z-Z, Luo S-J, Guo R-B. Experimental study on hydrate-based CO_2 removal from CH_4/CO_2 mixture. Energy 2016;104:76–84. https://doi.org/10.1016/j.energy.2016.03.107.
[21] Lim J, Choi W, Mok J, Seo Y. Kinetic CO_2 selectivity in clathrate-based CO_2 capture for upgrading CO_2-rich natural gas and biogas. Chem Eng J 2019;369:686–93. https://doi.org/10.1016/j.cej.2019.03.117.
[22] Cheng Z, Liu W, Li S, Wang S, Liu Y, Sun X, et al. High-efficiency separation of CO_2 from CO_2-CH_4 gas mixtures via gas hydrates under static conditions. Sep Purif Technol 2022;296:121297. https://doi.org/10.1016/j.seppur.2022.121297.
[23] Iino K, Takeya S, Ohmura R. Characterization of clathrate hydrates formed with CH_4 or CO_2 plus tetrahydropyran. Fuel 2014;122:270–6. https://doi.org/10.1016/j.fuel.2014.01.040.
[24] Lee Y-J, Kawamura T, Yamamoto Y, Yoon J-H. Phase equilibrium studies of tetrahydrofuran (THF) + CH_4, THF + CO_2, CH_4 + CO_2, and THF + CO_2 + CH_4 hydrates. J Chem Eng Data 2012;57:3543–8. https://doi.org/10.1021/je300850q.
[25] Seo D, Lee S, Lee Y, Park Y. Tailoring gas hydrate lattice dimensions for enhanced methane selectivity in biogas upgrading. Chem Eng J 2023;472:145079. https://doi.org/10.1016/j.cej.2023.145079.
[26] Horii S, Ohmura R. Continuous separation of CO_2 from a $H_2 + CO_2$ gas mixture using clathrate hydrate. Appl Energy 2018;225:78–84. https://doi.org/10.1016/j.apenergy.2018.04.105.
[27] Misawa T, Ishikawa T, Takeya S, Alavi S, Ohmura R. Continuous hydrate-based CO_2 separation from $H_2 + CO_2$ gas mixture using cyclopentane as co-guest. J Ind Eng Chem 2023;121:228–34. https://doi.org/10.1016/j.jiec.2023.01.026.
[28] Maruyama M, Kao S, Kiyokawa H, Takeya S, Ohmura R. Continuous CO_2 separation from a $N_2 + CO_2$ gas mixture using clathrate hydrate: insights into sustainable post-combustion carbon capture. Energy Fuels 2022;36:10601–9. https://doi.org/10.1021/acs.energyfuels.2c01355.
[29] Akatsu S, Tomita S, Mori YH, Ohmura R. Thermodynamic simulations of hydrate-based removal of carbon dioxide and hydrogen sulfide from low-quality natural gas. Ind Eng Chem Res 2013;52:15165–76. https://doi.org/10.1021/ie402010p.
[30] Tsuji H, Ohmura R, Mori YH. Forming structure-H hydrates using water spraying in methane gas: effects of chemical species of large-molecule guest substances. Energy Fuels 2004;18(2):418–24. https://doi.org/10.1021/ef034054g.
[31] Zhang S, Gao S, Yuan P, Yang Z, Ma Y, Ge X, et al. High-resolution VOCs measurements and photochemical impact analysis for typical solid waste base in summer. Air Qual Atmos Health 2025;18:1973–91. https://doi.org/10.1007/s11869-025-01746-z.
[32] W. Wang, J. Shen, Y. Chen, D. Zheng, L. Li, Identification and analysis of volatile organic compound and very volatile organic compound of MDF coated with different lacquers and their health risks to humans, J Env Chem Eng 12 (2024) 2, 112120. https://doi.org/10.1016/j.jece.2024.112120.
[33] Izumi F, Momma K. Three-dimensional visualization in powder diffraction. Solid State Phenomen 2007;130:15–20. https://doi.org/10.4028/www.scientific.net/SSP.130.15.
[34] Mori YH, Komae N. A note on the evaluation of the guest-gas uptake into a clathrate hydrate being formed in a semibatch- or batch-type reactor. Energy Conv Managem 2008;49(5):1056–62. https://doi.org/10.1016/j.enconman.2007.09.017.

[35] Yasuda H, Uenoyama Y, Nobuta O, Kobayashi S, Ryu I. Radical chain reactions using THP as a solvent. Tetrahedron Lett 2008;49:367–70. https://doi.org/10.1016/j.tetlet.2007.11.039.
[36] Matsubara H, Suzuki S, Hirano S. An *ab initio* and DFT study of the autoxidation of THF and THP. Org Biomol Chem 2015;13:4686–92. https://doi.org/10.1039/C5OB00012B.
[37] Yamamoto K, Iwai T, Hiraga K, Miyamoto T, Hotta A, Ohmura R. Synthesis and thermophysical properties of Tetrabutylammonium picolinate hydrate as an energy storage phase change material for cold chain. J Energy Storage 2022;55:105812. https://doi.org/10.1016/j.est.2022.105812.
[38] Gholinezhad J, Chapoy A, Tohidi B. Separation and capture of carbon dioxide from CO_2/H_2 syngas mixture using semi-clathrate hydrates. Chem Eng Res Des 2011;89(9):1747–51. https://doi.org/10.1016/j.cherd.2011.03.008.
[39] Kim SM, Lee JD, Lee HJ, Lee EK, Kim Y. Gas hydrate formation method to capture the carbon dioxide for pre-combustion process in IGCC plant. Int J Hydrogen Energy 2011;36(1):1115–21. https://doi.org/10.1016/j.ijhydene.2010.09.062.
[40] Babu P, Chin WI, Kumar R, Linga P. Systematic evaluation of tetra-n-butyl ammonium bromide (TBAB) for carbon dioxide capture employing the clathrate process. Ind Eng Chem Res 2014;53(12):4878–87. https://doi.org/10.1021/ie4043714.
[41] Pan M, Luzi-Helbing M, Schicks JM. Heterogeneous and coexisting hydrate phases - formation under natural and laboratory conditions. Energy Fuels 2022;36(18):10489–503. https://doi.org/10.1021/acs.energyfuels.2c01326.
[42] Maruyama M, Horsfield B, Spangenberg E, Ohmura R, Schicks JM. Interactions between gas hydrate and hydrogen in nature: laboratory evidence of hydrogen incorporation. Int J Hydrogen Energy 2025;184:151927. https://doi.org/10.1016/j.ijhydene.2025.151927.
[43] Narayanan TM, Imasato K, Takeya S, Alavi S, Ohmura R. Structure and guest dynamics in binary clathrate hydrates of tetrahydropyran with carbon dioxide/methane. J Phys Chem C 2015;119:25738–46. https://doi.org/10.1021/acs.jpcc.5b08220.
[44] Udachin KA, Ratcliffe CI, Ripmeester JA. Single crystal diffraction studies of structure I, II and H hydrates: structure, cage occupancy and composition. J Supramol Chem 2002;2(4–5):405–8. https://doi.org/10.1016/S1472-7862(03)00049-2.
[45] Darbouret M, Cournil M, Herri J-M. Rheological study of TBAB hydrate slurries as secondary two-phase refrigerants. Int J Refrigeration 2005;28:663–71. https://doi.org/10.1016/j.ijrefrig.2005.01.002.
[46] Nakayama T, Tomura S, Ozaki M, Ohmura R, Mori YH. Engineering investigation of hydrogen storage in the form of clathrate hydrates: conceptual design of hydrate production plants. Energy Fuels 2010;24:2576–88. https://doi.org/10.1021/ef100039a.
[47] Hatsugai T, Nakayama R, Tomura S, Akiyoshi R, Nishitsuka S, Nakamura R, et al. Development and continuous operation of a bench-scale system for the production of $O_3 + O_2 + CO_2$ hydrates. Chem Eng Technol 2020;43:2307–14. https://doi.org/10.1002/ceat.202000044.
[48] Hatsugai T, Kiyokawa H, Takeya S, Ohmura R. Improved operation of continuous ozone hydrate production. Chem Eng Technol 2021;44:1677–85. https://doi.org/10.1002/ceat.202100071.
[49] Maruyama M, Tomura S, Yasuda K, Ohmura R. Zero emissions, low-energy water production system using clathrate hydrate: engineering design and techno-economic assessment. J Clean Prod 2023;383:135425. https://doi.org/10.1016/j.jclepro.2022.135425.